Exact linear response of reacting thermal defects driven by creation processes

C. P. Flynn

Physics Department and Materials Research Laboratory, University of Illinois at Urbana-Champaign, Urbana, Illinois 61801, USA

(Received 5 December 2006; revised manuscript received 12 February 2007; published 23 April 2007)

The exact, linear response at steady state is calculated for reacting, but otherwise noninteracting, thermal defects driven by defect creation processes. The theory applies to vacancies and interstitials in the bulk, or to adatoms and advacancies on surface terraces. A wide variety of possible driving forces includes nuclear reaction, particle irradiation, epitaxial growth, surface erosion, and sublimation. When the defect life cycle typically starts and ends with spontaneous pair creation and annihilation, both species respond to the *difference* of their separate driving terms (the "Poisson" regime), and the law of mass action holds everywhere with a position dependent chemical potential $\mu^*(\mathbf{r})$. The value of $\mu^*(\mathbf{r})$ in linear response is employed here to discuss the conditions under which thermal defects precipitate, particularly as islands on terraces and dislocation loops in the bulk. It is shown, for the Poisson regime, that an approximate symmetry exists between processes for the two antidefects. Specifically, if μ_c^* suffices to nucleate a precipitate of one antidefect, then $-\mu_c^*$ is required to nucleate the other.

DOI: 10.1103/PhysRevB.75.134106 PACS number(s): 61.72.Ji, 61.72.Cc, 61.80.Az, 68.35.Fx

I. INTRODUCTION

In crystalline solids, the flow of matter by reaction or diffusion is mediated by thermal point defects.[1–3] Bulk metals support reacting antidefects that are vacancies and interstitials, of which the former generally determine behavior close to equilibrium.[1,2] On the surfaces of crystals, the antidefects are advacancies and adatoms, of which the latter are thought to be dominant on many metal surfaces.[4–7] (Such surface and bulk processes are not, in reality, entirely distinct but rather are linked by specific mixed reactions in a way described elsewhere).[8] A variety of interesting phenomena occur when a system of defects is driven by an external agency.[9–11] When unperturbed, thermal point defects are created and annihilate at fixed sinks such as dislocations and surface steps; antidefect pairs also form and annihilate spontaneously in translationally invariant crystal, either surface or bulk. These are the processes by which thermal defects establish their equilibrium concentrations, when their chemical potential μ is zero. When an external force creates additional defects, the defect system is driven from equilibrium, and the chemical potential remote from fixed sinks then generally differs from zero. Under these conditions thermal point defects may nucleate new sinks at which the excess population precipitates. In the present paper, these phenomena are treated comprehensively within a single linear formulation that becomes exact for small perturbations. In application to practical cases it often turns out that precipitation does indeed require only small changes of defect chemical potential.[12]

The processes of interest here take place under a variety of circumstances that have received earlier experimental attention. They occur, for example, when interstitials nucleate and precipitate out as dislocation loops in irradiated metals and semiconductors.[13] Exotic cases for bulk vacancies are exemplified by precipitation in quenched metals as stacking fault tetrahedra,[14] or as a spatially extended "void lattice"[15] from supersaturation in a material driven by irradiation. In the area of surface science, the creation of surface islands of both signs is observed in the erosion and the epitaxial growth of crystals by means of ion beams.[16,17] Very similar structures result when atoms sublime from surfaces into vacuum at elevated temperatures, and so this drives the system from equilibrium.[18,19]

Nucleation of precipitates from supersaturated solution, and the flow of reacting species to these and other sinks, are topics that possess extensive literatures. A current treatment of processes in irradiated alloys, with references to earlier studies, is given by Doan and Martin.[20] A treatment of surfaces during sublimation is given by Pimpinelli and Villain,[12] together with earlier experimental literature. Several works treat the molecular dynamics of ion beam impacts on crystal surfaces,[11,21] including nucleation of sinks, but generally omit subsequent long term equilibration.

The present research was undertaken to place these several processes in a unified context. The goal is to treat driven defect systems exactly, for the limit of small driving forces. The linear response of the chemical potential μ^* to the driving force may then be obtained precisely, and this may suffice to determine the nucleation of precipitates also. As mentioned above, precipitation of thermal defects occurs for rather small changes of chemical potential, and so a linear theory may find wide practical use.

The present discussion proceeds on the basis of two recent advances. First, exact equations that describe the reacting (but otherwise noninteracting) system of antidefects in the simultaneous presence of fixed sinks and driving forces have been linearized and solved generally for the homogeneous limit in which driving terms are negligible.[22] The inclusion of a driving force requires, in addition, particular integrals for the linearized equations. General results for the driven steady state are presented below for the case in which the driving force is spatially uniform. These have practical value because defect creation is often quite uniform in cases of nuclear decay, ion beam irradiation, and of sublimation. The equations remain symmetrical between the two species of antidefect and may be solved to obtain their self-consistent linear disturbances.

The chemical potential can be derived from these concentrations. A second recent advance pertinent here is the recognition[22] that a reacting defect system has a chemical potential μ^* and temperature T^* of its own, generally different from those of the embedding lattice, namely μ and T. In particular, the quantity μ^* determines the size and sign of the driving force for defect precipitation in the present treatment of strongly reacting antidefects.

In what follows, the necessary equations are gathered in Sec. II A, and solved in Sec. II B, with application to geometries of interest deferred to Appendix A. The topic of Sec. III is the resulting chemical potential and its characteristics in several well-defined limits. For strongly reacting systems these include a "Poisson" regime in which driving forces create a substantial excess of one defect species, and a "Frenkel pair" regime in which the two species form at comparable rates. For weaker reactions, relative to diffusion, the Poisson regime has different characteristics. Section IV then considers applications of the results to precipitation of driven defects. For the strongly reacting Poisson regime, this includes a predicted symmetry between driven precipitation of the two defects separately. The distributions of precipitates expected in the several limiting regimes of behavior are discussed in Appendix E.

II. LINEAR RESPONSE IN DRIVEN SYSTEMS OF THERMAL POINT DEFECTS

A. Basic equations

In this work we treat surface and bulk processes as separate phenomena in their respective two- and three-dimensional domains, neglecting the coupling caused by transitions in which defects hop between surface and bulk sites.[8] Within this limitation, the defect processes of interest here may be treated without specifying the particular geometry of concern. By $c_1(\mathbf{r},t)$ we designate the occupation probabilities of defect sites containing an added atom (interstitial or adatom in the two cases) and by $c_2(\mathbf{r},t)$ the occupation of sites with missing atoms (vacancy or advacancy). The equilibrium values $\bar{c}_1,\bar{c}_2$, of these quantities are constants in unperturbed systems at a fixed temperature.

The equations that determine the rate at which the c change with time are[22]

$$\dot{c}_1 - D_1\nabla^2(c_1-\bar{c}_1) - K_{12}(\bar{c}_1\bar{c}_2 - c_1c_2) = K_1(\mathbf{r},t); \quad (1a)$$

$$\dot{c}_2 - D_2\nabla^2(c_2-\bar{c}_2) - K_{12}(\bar{c}_1\bar{c}_2 - c_1c_2) = K_2(\mathbf{r},t). \quad (1b)$$

Here, rate constants are, by convention,[23] written as K. K_1 is the position- and time-dependent rate, per added-atom site, at which defects are created by external agencies; K_2 is the analogous quantity for missing-atom sites. K_{12} is the rate constant for antidefect reaction, with $K_{12}\bar{c}_1\bar{c}_2$ the rate per lattice site at which pairs are created, and $K_{12}c_1c_2$ the annihilation rate. D_1 and D_2 are the hopping diffusion coefficients[8] of the two species, so that the first two terms of Eqs. (1a) and (1b) comprise the diffusion equation for the excess of a species, in the absence of reactions and driving terms. Note that Eqs. (1) are written for a lattice in which vacancy defects and added atom defects have equally numerous sites; cases with different site densities can be accommodated with more elaborate notation.

It is important that the reaction terms in Eqs. (1a) and (1b) are identical, so that

$$\nabla^2(D_1c_1 - D_2c_2) = K_2 - K_1 \quad (2)$$

holds everywhere for the steady state (when the c_i lack time dependence). At fixed sinks where $c_i \to \bar{c}_i$ for both species, and thus $\dot{c}_i \to 0$, the boundary conditions are evidently

$$-\nabla^2 D_1c_1 = K_1; \quad -\nabla^2 D_2c_2 = K_2 \quad (3)$$

(at fixed sinks, regardless of time-dependent forces).

In this paper we treat weak perturbing forces for which the defect concentrations undergo only small fractional changes. The nonlinear Eqs. (1) may be linearized by writing $c_1=\bar{c}_1+s_1$; $c_2=\bar{c}_2+s_2$. Then

$$\left[\frac{\partial}{\partial t} - D_1\nabla^2 + K_{12}\bar{c}_2\right]s_1 = -K_{12}\bar{c}_1s_2 + K_1(\mathbf{r},t);$$

$$\left[\frac{\partial}{\partial t} - D_2\nabla^2 + K_{12}\bar{c}_1\right]s_2 = -K_{12}\bar{c}_2s_1 + K_2(\mathbf{r},t). \quad (4)$$

With nonlinear terms in c_1,c_2 eliminated, Eqs. (4) become linear in s_1, s_2. They are to be solved simultaneously subject to boundary condition (see above):

$$s_i = 0; \quad \nabla^2 s_i = -K_i/D_i, \quad (5)$$

at fixed sinks, where $c_i=\bar{c}_i$.

A general comment on regimes of behavior for Eqs. (1) in the driven steady state may be helpful here. With time dependence eliminated, the response may reasonably be named *diffusion dominated* when the term on the left containing D is larger than that containing K_{12}, and *reaction dominated* in the opposite case. The former regime may remain linear for large perturbations, but linear response in the reaction dominated regime is clearly limited to driving forces K_i such that $K_i < K_{12}\bar{c}_1\bar{c}_2$. Otherwise the term $K_{12}(c_1c_2-\bar{c}_1\bar{c}_2)$ cannot possibly remain linear in the perturbations s_1, s_2 of the equilibrium defect densities.

B. The steady state of linear response to uniform driving forces

Here we find general solutions for Eqs. (4) for specific impressed conditions. The relevant conditions are (a) that the driving terms K_1 and K_2 are constants, specifically uniform in space, and time-independent; and (b) that the system is studied in the steady state of response to these driving terms. Then, setting $\partial/\partial t \to 0$ we find

$$[-D_1\nabla^2 + K_{12}\bar{c}_2]s_1 = -K_{12}\bar{c}_1s_2 + K_1;$$

$$[-D_2\nabla^2 + K_{12}\bar{c}_1]s_2 = -K_{12}\bar{c}_2s_1 + K_2. \quad (6)$$

It follows that

$$[2][1]s_1 = [2](-K_{12}\bar{c}_1 s_2 + K_1) = -K_{12}\bar{c}_1(-K_{12}\bar{c}_2 s_1 + K_2) + K_{12}\bar{c}_1 K_1, \quad (7)$$

in which, for brevity, the operators in brackets from Eqs. (6) are written [1], [2]. Equations (6) can now be separated to leave

$$[D_1 D_2 \nabla^4 - (D_1\bar{c}_1 + D_2\bar{c}_2)K_{12}\nabla^2]s_1 = K_{12}\bar{c}_1(K_1 - K_2);$$

$$[D_1 D_2 \nabla^4 - (D_1\bar{c}_1 + D_2\bar{c}_2)K_{12}\nabla^2]s_2 = K_{12}\bar{c}_2(K_2 - K_1). \quad (8)$$

We can find s_1, s_2 in general as follows. The quantity $\sigma_1 = \nabla^2 s_1$ satisfies the equation

$$(\nabla^2 - \kappa^2)\sigma_1 = \lambda_1, \quad (9)$$

in which

$$\kappa^2 = K_{12}(D_1\bar{c}_1 + D_2\bar{c}_2)/D_1 D_2; \quad \lambda_1 = K_{12}\bar{c}_1(K_1 - K_2)/D_1 D_2. \quad (10)$$

This is the wave equation for imaginary eigenvalue,[24] κ, to be solved subject to the boundary condition, from Eqs. (5), of $\sigma_1 = -K_1/D_1$ at fixed sinks. Suppose that, for any particular sink geometry, the eigenfunction of the wave equation $(\nabla^2 - \kappa^2)\gamma(\mathbf{r}) = 0$, with $\gamma = 1$ at fixed sinks, is $g_\kappa(\mathbf{r})$. The solution $\sigma_1 = -\lambda_1/\kappa^2 + A\ g_\kappa(\mathbf{r})$, of Eq. (9), with A in general an arbitrary constant, is now found from the boundary condition as

$$D_1\sigma_1(\mathbf{r}) = -K_1 + A[g_\kappa(\mathbf{r})/g_\kappa(\rho) - 1]; \quad (11a)$$

$$D_2\sigma_2(\mathbf{r}) = -K_2 + A[g_\kappa(\mathbf{r})/g_\kappa(\rho) - 1], \quad (11b)$$

with

$$A = -\frac{D_1\bar{c}_1 K_2 + D_2\bar{c}_{12}K_1}{D_1\bar{c}_1 + D_2\bar{c}_{12}}. \quad (12)$$

With $\sigma_1 = \nabla^2 s_1$, the general solutions now follow as

$$D_1 s_1 = \frac{D_1\bar{c}_1(K_2 - K_1)}{D_1\bar{c}_1 + D_2\bar{c}_2} f(\mathbf{r}) + \frac{A}{\kappa^2}\left[\frac{g_\kappa(\mathbf{r})}{g_\kappa(\rho)} - 1\right],$$

$$D_2 s_2 = \frac{D_2\bar{c}_2(K_1 - K_2)}{D_1\bar{c}_1 + D_2\bar{c}_2} f(\mathbf{r}) + \frac{A}{\kappa^2}\left[\frac{g_\kappa(\mathbf{r})}{g_\kappa(\rho)} - 1\right], \quad (13)$$

in which $f(\mathbf{r})$ is the solution of the Poisson equation $\nabla^2 f = 1$ that has $f(\mathbf{r}) = 0$ for the fixed sinks at $\mathbf{r} = \boldsymbol{\rho}$, and with $(\nabla^2 - \kappa^2)g(\mathbf{r}) = 0$, with $g = 1$ at fixed sinks. It may be verified by inspection that Eqs. (13) are solutions of $(\nabla^2 - \kappa^2)\nabla^2 s_i = \lambda_i$ that satisfy the desired boundary conditions $s = 0$ and $\nabla^2 s_i = -K_i/D_i$ for fixed sinks at $\mathbf{r} = \boldsymbol{\rho}$. Specific solutions for some cases with simple geometries are presented in Appendix A.

The form of these solutions is of some general interest. Under conditions where reactions are dominant (K_{12} and hence κ, large), the second term on the right in Eqs. (13) may be neglected and the solutions become

$$s_1 = \frac{\bar{c}_1(K_2 - K_1)}{D_1\bar{c}_1 + D_2\bar{c}_2} f(\mathbf{r}); \quad s_2 = \frac{\bar{c}_2(K_1 - K_2)}{D_1\bar{c}_1 + D_2\bar{c}_2} f(\mathbf{r}). \quad (14)$$

As now $s_1/\bar{c}_1 = -s_2/\bar{c}_2$, Eqs. (14) correspond to the system at equilibrium with a changed chemical potential $\mu^*(\mathbf{r}) = k_B T s_1(\mathbf{r})/\bar{c}_1$. Note that the system responds only to the *difference* of the creation rates K_1, K_2 because, in this limit, all other excess defects annihilate by reaction, and only this difference reaches the fixed sinks.

In the opposite limit, $\kappa \to 0$, in which reactions become negligible, $\kappa^{-2}[g_\kappa(\mathbf{r})/g_\kappa(\rho) - 1] \to f(\mathbf{r})$, and from Eqs. (13),

$$D_1 s_1 = -K_1 f(\mathbf{r}); \quad D_2 s_2 = -K_2 f(\mathbf{r}), \quad (15)$$

so that the two species of antidefect diffuse to the sinks independently. It is certainly of interest that these are solutions of the Poisson equation in both the fast reaction and slow reaction limits, but with differing driving terms.

A further limit is reached when $K_1 = K_2 = K$, and the first (Poisson) term in the response vanishes identically. Then the driving process creates only Frenkel pairs. The exact linear response is

$$D_1 s_1 = D_2 s_2 = \frac{K}{\kappa^2}\left[1 - \frac{g_\kappa(r)}{g_\kappa(\rho)}\right]. \quad (16)$$

Hence in the limit of weak reaction (κ small) we recover Eqs. (15) with $K_1 = K_2$, while for κ large the result is

$$D_1 s_1 = D_2 s_2 = \frac{\mathrm{K}D_1 D_2}{K_{12}(D_1\bar{c}_1 + D_2\bar{c}_2)}\left[1 - \frac{g_\kappa(r)}{g_\kappa(\rho)}\right]. \quad (17)$$

It will normally be the case that one defect dominates mass diffusion so that, say, $D_1\bar{c}_1 \gg D_2\bar{c}_2$. Then with $K_1 = K_2 = K$, for $\mathbf{r}$ far from $\boldsymbol{\rho}$, where $g_\kappa(\mathbf{r})/g_\kappa(\boldsymbol{\rho}) \to 0$ in the limit of strong reactions for which κ is large,

$$s_1 = \frac{\mathrm{K}D_2}{K_{12}D_1\bar{c}_1}; \quad s_2 = \frac{K}{K_{12}\bar{c}_1}, \quad (18)$$

and analogous results when $D_2\bar{c}_2 \gg D_1\bar{c}_1$. A notable point, to which we return below, is that the concentration of the *nondominant* defect may exhibit a larger *absolute* increase than that of the dominant defect [see Eqs. (18)] under these circumstances. The *fractional* increase, $s_2/\bar{c}_2 = K/K_{12}\bar{c}_1\bar{c}_2$, is evidently the ratio of rate, per site, of driven defect creation, to the rate of spontaneous creation, whereas $s_1/\bar{c}_1$ is smaller by a factor $D_2\bar{c}_2/D_1\bar{c}_1$. This is the ratio of the mass diffusion coefficients. The reverse result holds when the minority and majority roles are exchanged.

III. CHEMICAL POTENTIAL IN THE DRIVEN SYSTEM

A. General concerns

Chemical processes such as precipitation or sublimation are responsive to the chemical potential of the defect system.[25,26] In the present context, the factors of concern in the chemical potential are not entirely trivial. When the reaction between antidefects is not significant, it is reasonable to treat the defects as entirely distinct, each with its own chemical potential:

$$\mu_1 = k_B T \ln(c_1/\bar{c}_1) \approx k_B T s_1/\bar{c}_1;$$

$$\mu_2 = k_B T \ln(c_2/\bar{c}_2) \approx k_B T s_2/\bar{c}_2, \tag{19}$$

with T the temperature of the embedding lattice. When, however, the reactions are important, the defect system as a whole can be ascribed[22] its own temperature, T^*, and chemical potential, μ^*, that, respectively, describe the ability of the defect system itself to provide heat energy and atoms to lattice sinks. The relevant quantities[22] are

$$T^* = T\frac{\ln \bar{c}_1\bar{c}_2}{\ln c_1 c_2}; \tag{20a}$$

$$\mu^* = \frac{k_B T}{2}\left[\frac{\ln \bar{c}_1\bar{c}_2 \ln(c_1/c_2)}{\ln c_1 c_2} - \ln(\bar{c}_1/\bar{c}_2)\right]$$
$$= (k_B T/2)[T^* \ln c_1 c_2 - T \ln \bar{c}_1\bar{c}_2], \tag{20b}$$

in which the second form of Eq. (20b) follows from use of Eq. (20a). These quantities are not intuitive in form, but correctly reduce to $T^*=T$ and $\mu^*=\mu$ in the limit $c_i \to \bar{c}_i$. More generally they determine arbitrary populations c_1, c_2 of two antidefects by a common temperature and chemical potential. T^* and μ^* are certainly the appropriate variables with which to describe the transfer of heat energy and particles between fixed sinks and a strongly reacting defect assembly.

One concern here is with nucleation processes that are dominated by μ^*. It is worth noting that $T^*=T$ for distributions given by Eqs. (14) with strong reactions (i.e., the law of mass action holds for a fixed temperature, T, common to the lattice and defects). The remainder of this section treats the chemical potential created by linear response in driven systems of reacting thermal defects.

B. Exact chemical potential in linear steady state response

To determine the linear response in μ^*, Eq. (20b) may be rewritten, with $c_i=\bar{c}_i(1+s_i/\bar{c}_i)$, and with the logarithms expanded, to obtain the first order result

$$\mu^* = \frac{k_B T}{2}\left[\frac{s_1}{\bar{c}_1} - \frac{s_2}{\bar{c}_2} - \frac{\ln(\bar{c}_1/\bar{c}_2)}{\ln \bar{c}_1\bar{c}_2}\left(\frac{s_1}{\bar{c}_1} + \frac{s_2}{\bar{c}_2}\right)\right]. \tag{21}$$

With the $c_i \ll 1$, the factor containing logarithms, $(\ln \bar{c}_1 - \ln \bar{c}_2)/(\ln \bar{c}_1 + \ln \bar{c}_2)$, is $\sim \pm 1$ when one antidefect exists in much larger concentrations than the other, and otherwise has still smaller magnitude. Also, for strong reactions, $s_1/\bar{c}_1 \approx -s_2/\bar{c}_2$, and these two facts then combine to make the last term on the right usually unimportant.

In full, the exact linear response obtained from Eqs. (13) for the s_i and Eq. (21) for μ^* is

$$\mu^*(\mathbf{r}) = B f(\mathbf{r}) + C\left[\frac{g_\kappa(\mathbf{r})}{g_\kappa(\rho)} - 1\right] \tag{22a}$$

with

$$B = \frac{k_B T(K_2 - K_1)}{D_1\bar{c}_1 + D_2\bar{c}_2}, \tag{22b}$$

and

$$C = \frac{k_B T(K_2 D_1\bar{c}_1 + K_1 D_2\bar{c}_2)}{2K_{12}\bar{c}_1\bar{c}_2(D_1\bar{c}_1 + D_2\bar{c}_2)} h(\bar{c}_1,\bar{c}_2), \tag{22c}$$

with

$$h(\bar{c}_1,\bar{c}_2) = \frac{D_1\bar{c}_1 - D_2\bar{c}_2}{D_1\bar{c}_1 + D_2\bar{c}_2} + \frac{\ln(\bar{c}_1/\bar{c}_2)}{\ln(\bar{c}_1\bar{c}_2)}. \tag{22d}$$

This response is linear in the driving forces K_i, as is appropriate for the limit under study. The term containing B corresponds to a perturbation that changes the chemical potential only, since $T^*=T$. The term in C incorporates corrections with $T^* \neq T$ close to sinks. From Eqs. (13) the term in $g(\mathbf{r})$ gives exactly compensating fluxes of the two antidefects. The added fluxes result in an increase of sink fluctuations[27] which, however, remain small in the linear regime. This matter is discussed further in Appendix C.

We continue by evaluating μ^* in terms of driving forces K_1, K_2, for strong reactions in general, and also for the special case of pure Frenkel pair creation, which has the special interest mentioned in Sec. II B.

1. $\mu^*(\mathbf{r})$ *for dominant reactions*

It is useful to understand the typical sizes of the competing terms in Eq. (22). For the regime in which reactions dominate the behavior (see Sec. II A), the system remains linear only when $K < K_{12}\bar{c}_1\bar{c}_2$, so that the defect creation by the driving forces does not overwhelm the dominant equilibrium pair creation. Also, both terms on the right of Eq. (22d) are of magnitude less than or equal to 1. These facts cause the term containing K_{12} to remain generally small compared to the first (Poisson) term [that contains $f(\mathbf{r})$] throughout almost the entire linear regime of μ^*. Here the Poisson term alone thus provides a useful approximation to the full result. It is an important point, in this limit of strong reactions, that the responses to K_1 and K_2 are precisely equal in amplitude and opposite in sign. Explicit functions $f(\mathbf{r})$ showing the response as a function of position, for specific examples with various geometries, are given below in Appendix A. Under other circumstances, when the second term on the right of Eq. (22a) does become significant, the response remains linear in each of the driving forces K_1, K_2, but the two responses generally differ to some extent in magnitude and in sign.

Since the Poisson portion of μ^* is dominant for strong reactions, a simple understanding of the behavior may be of value in an experimental context. Rather than divert the discussion here, the matter is deferred to Appendix B. There it is shown how behavior in the Poisson limit is consistent with a simple perspective, in which those defects that remain after reaction, drain off to sinks in accordance with predictions of the Nernst-Einstein equation.

2. *Chemical potential in the diffusion-dominated regime*

It is generally believed that, in most bulk metals up to the melting temperature T_m, and on metal surfaces below $\sim T_m/3$, thermal defects are created predominantly at fixed sinks.[22] The typical life span of a defect then consists of

passage by diffusion from the sink at which it is created to the sink at which it eventually annihilates. Reactions among antidefects thus play a minor role, and it becomes necessary to consider the two antidefects as possessing their independent chemical potentials, $\mu_i = k_B T \ln(c_i/\bar{c}_i)$, separately.

The required results follow directly from Eqs. (15) by linearizing the logarithmic terms as

$$\mu_1(\mathbf{r}) = \frac{k_B T K_1}{D_1 \bar{c}_1} f(\mathbf{r}); \quad \mu_2(\mathbf{r}) = \frac{k_B T K_2}{D_2 \bar{c}_2} f(\mathbf{r}). \tag{23a}$$

Evidently the response no longer depends only on $K_1 - K_2$, and instead the two species respond differently to their separate driving forces. Indeed for large driving forces for each antidefect it is possible that both may simultaneously exceed whatever criterion determines the onset of nucleation. The form taken by the chemical potentials can again be readily understood from the Nernst-Einstein relationship (see Appendix B).

Outside the linear regime, when the driving forces are large, the result

$$\mu_i = k_B T \ln \bar{c}_i [1 + K_i f(\mathbf{r})/D_i \bar{c}_i], \tag{23b}$$

with $i=1$ or 2, remains valid up to K_i sufficiently large that $\kappa R \sim 1$, whereupon the c_i are both reduced by reaction. Note also that the response $\mu(\mathbf{r})$ no longer remains a solution of Poisson's equation in this extended regime, because the term in f is in the argument of the logarithm.

3. μ^* for pure Frenkel pair creation

When $K_1 = K_2 = K$, the Poisson term in $\mu(\mathbf{r})$ is exactly zero and, contrary to the conditions described above, the second term on the right of Eq. (22) assumes importance. Where the second term is significant, the ratio of the two terms is $\kappa^2 R^2 \Delta K/K$ with ΔK the difference between K_1 and K_2. In this regime, the driving forces create the two antidefects at equal rates, and a sufficiently fast reaction could then completely suppress defect density changes. From Eqs. (22) one then has

$$\mu(\mathbf{r}) = \frac{k_B T K}{2 K_{12} \bar{c}_1 \bar{c}_2} \left[\frac{D_1 c_1 - D_2 \bar{c}_2}{D_1 c_1 + D_2 \bar{c}_2} + \frac{\ln \bar{c}_1 - \ln \bar{c}_2}{\ln \bar{c}_1 + \ln \bar{c}_2} \right] \left[\frac{g_\kappa(r)}{g_\kappa(\rho)} - 1 \right]. \tag{24}$$

As explained in what follows, the first concentration-dependent term in the braces has the effect of stabilizing *dominant* defects and destabilizing the minority species. Often, one species will dominate transport, and the term in question is then approximately ±1, taking the sign of the dominant defect: i.e., +1 for $D_1 \bar{c}_1 \gg D_2 \bar{c}_2$, and −1 for the opposite case. Since the r-dependent factor is everywhere negative, the first term of the factor in braces, for a positive force K, drives μ negative, which destabilizes the minority species. To the contrary, the second term, containing logarithms of small quantities $\ll 1$, creates the opposite trend. The two terms are evaluated approximately in Sec. III C for reasonable models to find that the first term dominates, and the net response has its sign and a magnitude between 0.5 and 1, relatively independent of T. The overall effect is that a system driven sufficiently hard at $K_1 = K_2$ eventually reaches a chemical potential of magnitude large enough to nucleate minority precipitates. The minority defects thus selected are then forced out of solution to some extent (see Sec. III C below).

These predictions are of practical interest. In most metals, vacancies are certainly the dominant defects both in site occupancy $\bar{c}$ and in mass transport $D\bar{c}$.[28] It is therefore of specific interest in the present connection that *interstitials* (the minority species) formed in Frenkel pairs of irradiated metals are well-known to precipitate out, usually to form dislocation loops ("interstitial loops").[9–11] Although as yet not fully verified by experiment, adatoms are believed to be the majority species on most surfaces[4–7] and advacancies the minority. It might therefore be anticipated from Eq. (24) that advacancy islands form on metal surfaces irradiated by ion beams of the "neutral energy" at which adatoms and advacancies are created in equal numbers. Here one recognizes that a beam of self-ions at low impact energies causes epitaxial *growth* on the crystal surface, while at high impact energies there occurs sputtering with a net *loss* of ions from the surface. In between these extremes lies the "neutral energy" at which there is neither net addition nor loss of ions from the surface, only the steady state creation of adatom-advacancy (Frenkel) pairs.

C. Bulk and surface behavior for a standard metal

To place the results for the chemical potential in perspective we evaluate some values for typical cases of pure bulk metals and for their typical close packed surfaces. It has recently been suggested[22] for both cases that all metals conform sufficiently well to an average model as to provide a useful guide for typical behavior. Values of $\bar{c}_i(T)$ and $D_i(T)$, that scale among metals as T/T_m, are reproduced for the reader's convenience in Appendix D. Here they are employed to illustrate typical behavior.

The inverse distance κ is important as it compares diffusion rates to reaction rates such that reactions dominate when $\kappa R \gg 1$, in which R is the system size (see Appendix A). The values of κ for bulk and surface of model metals are shown in Fig. 1. For surface systems with sinks (usually steps) spaced $\sim$10 nm apart, reactions dominate above $\sim T_m/4$, whereas, for the bulk, reactions dominate only for $R \sim 10\ \mu m$, even at T_m.

In the Frenkel pair regime, the magnitude of $\mu^*(r)$ varies in proportion to the function $h(T)$ in Eq. (22d). This is the sum of two terms which, respectively, contain mass diffusion coefficients, $D_i \bar{c}_i$, and the equilibrium concentrations $\bar{c}_i$. Figure 2 shows these terms, marked 1 and 2, evaluated for metal surfaces (solid lines) and for the bulk (dashed lines) as a function of T/T_m, for the standard parameters given in Appendix D. The totals, marked T, and given as heavy lines, are fairly independent of temperature and of magnitude typically between 0.5 and 1. With these parameters, the surface (positive) and bulk (negative) totals have opposite signs because adatoms dominate transport on surfaces whereas vacancies dominate mass transport in the bulk metal.

Interest centers also on the typical magnitude of the Poisson term relative to the Frenkel pair term. As mentioned

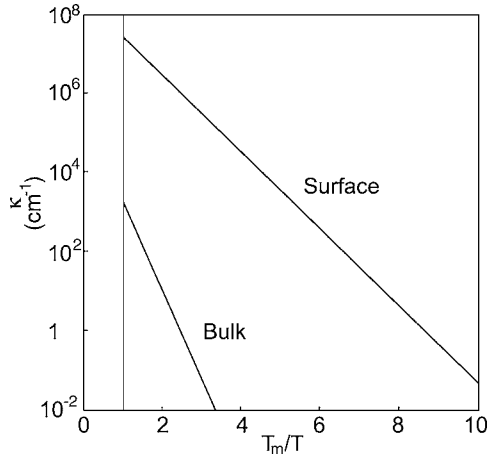

FIG. 1. Using defect parameters collected in Appendix B, the figure shows values of the reaction wave vector κ [Eq. (10)] for surface and bulk systems. For $\kappa R \gg 1$, with R the system size, thermal defect lifetimes are dominated by pair creation and annihilation, rather than to processes at fixed sinks.

above, the ratio in the region $K_1 \sim K_2$ is given approximately by $\kappa^2 R^2 \Delta K/K$ with $\Delta K = K_1 - K_2$. More generally, $(\kappa R)^2$ gives a typical order of magnitude for the relative size, and consequently κR gives the relative gradients.

IV. NUCLEATION OF THERMAL DEFECT PRECIPITATES

The results for steady state linear response of a driven defect system, presented above, may find applications in various practical cases of precipitation including, for example, those that include driving forces for defect creation due to epitaxial growth, erosion, fusion, fission, particle irradiation, sublimation, and so on. Precipitates nucleate when the chemical potential of the defects becomes unfavorable relative to that in the precipitate. Given an accurate theory of nucleation, the expressions for μ^* derived above then provide precisely the information needed to predict the conditions under which precipitates nucleate in terms of the driving forces applied to the reacting assembly. This requires that values of μ^* be inserted into equations that determine the nucleation rate.[25,26] It is not, however, clear at present that nucleation theory is fully predictive in any single case. In any event, results are particular to the case studied, and will not be considered here, leaving full development for specific applications to specialized works. Here we consider instead two generic features of the behavior. These include, first, a symmetry for strong reactions between behavior for the two antidefects; and second, the typical magnitude of μ^* required for nucleation of defect precipitates on metal surfaces and in their bulk. A related topic, concerning the spatial distribution of precipitates throughout the driven volume occupied by the reacting defect assembly, is deferred to Appendix E.

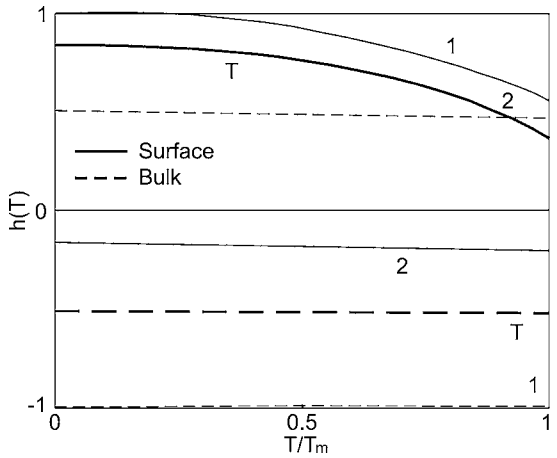

FIG. 2. Values of $h(T)$ from Eq. (23d), obtained using defect parameters from Appendix B. These determine the sign and size of the Frenkel pair term in $\mu^*(r)$.

A. Precipitation of thermal defects

Precipitation of particles from a random assembly takes place, in principle, when the chemical potential of the particles exceeds a critical value required to nucleate the new structure. Once nucleated, the precipitates driven by the chemical potential grow in size without bounds. A large literature[25,26,12] explores the character of the required critical nucleus and the rate at which nuclei form in the equilibrating precursor configuration for which the particles are dispersed in a macroscopically homogeneous fashion. Dimensionality enters into the process largely through the available distribution of nucleus geometries as a function of cluster size. A useful paper by Pimpinelli and Villain[12] offers a careful discussion of the case $d=2$ for comparison with $d=3$, with the altered distribution of cluster distribution $d=2$ entails. The central features of (i) a critical size of nucleus that separates transient clusters from those that grow; and (ii) growth[25,26] and fluctuation[27] by attachment of new particles through diffusion, remains common to the two cases. For this reason it remains possible to conduct the discussion with some generality.

Precipitation theory was developed for atoms in solution. Our present interest is focused on thermal defects and, unlike atoms, these are not independently conserved at fixed sinks. New features that require a separate discussion are thereby introduced. As a practical matter, defects tend to precipitate into disks one atom thick, as sketched in Fig. 3, and for clarity we confine the discussion to precipitates having this geometry. In the three-dimensional (3D) bulk, such precipitates occur as dislocation loops that form a finite region in which a new atomic plane nucleates between existing planes of the perfect crystal, or in which vacancies aggregate on a plane to eliminate a finite area of that plane [see Fig. 3(a)]. In either case the perimeter of the disk is an edge dislocation, and the area may or may not contain a stacking fault. For 2D terraces, precipitates include islands either of vacancies ("lacunae" or "Lochkeime"[18,19,29]) or of adatoms; in either case the perimeter of the island is a step edge, as in Fig. 3(b).

Precipitates occur more generally in a variety of differing geometries, not discussed here. Specifically, 3D loops may include a stacking fault in which planes occur out of sequence; other geometries include stacking fault tetrahedra and almost spherical voids. Here we consider 2D islands and 3D dislocation loops.

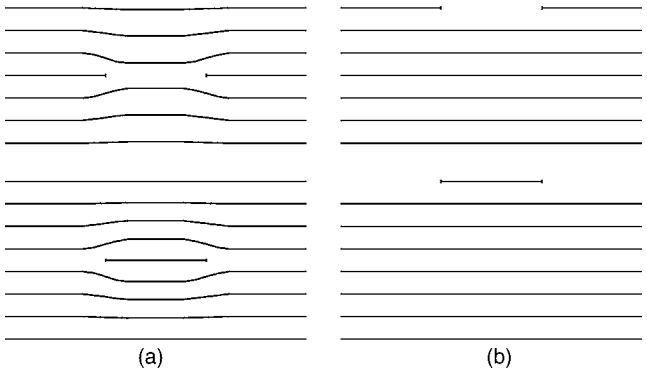

FIG. 3. Dislocation loops (left) and islands on a terrace (right) are dominant precipitates for vacancy-type (top) and added-atom defects (bottom) for bulk and surface systems.

Two features of the precipitation process for thermal defects require a particular note. First, a precipitate containing n thermal defects of species 1 can grow to size $n+1$ either by absorbing a further type 1 defect or by emitting a type 2 thermal defect. Complementary remarks apply to shrinking of type 1 precipitates and to growth or shrinking of type 2 precipitates. This behavior lies in clear distinction to impurity cases in which growth and shrinking of nuclei are associated specifically with addition and emission of impurities, respectively. The important consequence, for systems in the reaction-dominated regime, is that the evolutions of nuclei for types 1 and 2 precipitates *both* are determined by the same mass transport coefficient $D_1\bar{c}_1+D_2\bar{c}_2$. This is the case because the flow of each species between solution and a nucleus is determined by the same chemical potential μ^*. In the contrary case that behavior is diffusion dominated, the flow to type 1 and type 2 nuclei is determined by transport coefficients $\bar{D}_1\bar{c}_1$ and $\bar{D}_2\bar{c}_2$, respectively, because the chemical potential gradients generally differ between the two species.

A second property of nuclei formed from thermal defects lends further symmetry to the occurrence of type 1 and type 2 precipitates. This is the fact that both types of precipitate comprise a perfect crystal encircled by an edge dislocation loop (or perfect terrace enclosed within a step edge, for the surface case). The result is that the energetics of nuclei for large size n become identical for the two species. This is illustrated in Fig. 4, in which the energy is shown as a function of precipitate radius. Note that added-atom loops are shown by positive r and vacancy loops by negative r. For a positive chemical potential μ^*, favoring type 1 precipitation, the energetics are shown on the left, and for negative μ^*, favoring type 2 precipitation, on the right. The faint parabolic lines indicate the chemical potential change as $n=\pi r^2/\Omega$ defects leave the solution, and the faint straight lines represent the free energy $2\pi r\beta$ of the perimeter, with β its energy per unit length. The heavy lines in the two figures represent the summed energies. The central point made here is that, in this macroscopic discussion, the cases of type 1 and type 2 defects have identical descriptions. For chemical potentials $\pm|\mu^*|$, energies are identical in the two cases. We emphasize that this symmetry holds only for reaction-dominated systems where μ^* is a property of the entire defect system. In diffusion dominated cases the flow links, instead, to the separate chemical potentials of the two species.

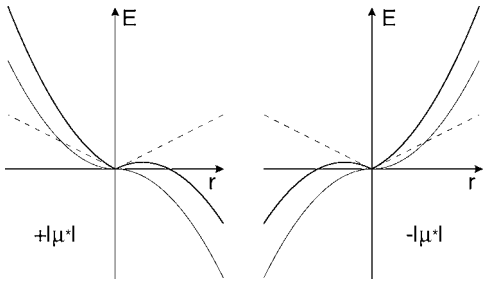

FIG. 4. Energetics of thermal defect precipitates. Radii of loops are indicated by r positive for added atom defects, and for vacancy loops by r negative. The nucleation barrier for added-atom defects when μ^* is positive (left) is then identical to the barrier for vacancy defects with the reverse μ^* (right). There results a symmetry between the two precipitation behaviors (see text).

A central result of this work for strongly reacting defect systems may now be stated. In the relevant limit, the chemical potential μ^* of the thermal defect system depends, through Eq. (22), only on the difference K_1-K_2 of the forces driving creation of the two species of thermal defect. In addition, the energetics of nucleation for the two species are identical for opposite values of μ^*. Finally, the kinetics of the two processes depend on the same transport coefficient $D_1\bar{c}_1+D_2\bar{c}_2$. Therefore we deduce that the entire precipitation processes for the two species must depend identically on the driving forces. Specifically, if the minimum creation rate $K=K_1-K_2$ is required to nucleate type 1 defects, then $-K$ is the minimum magnitude of differential creation required to nucleate type 2 precipitates. This is a general prediction for thermal defect precipitation from driven systems of reaction-dominated thermal defects in the Poisson regime.

In reality, of course, some residual asymmetry of energetics must be present for small n because the binding energies of small clusters certainly differ to some extent between the two species. The degree to which this symmetry breaking affects actual nucleation has not been determined at the present time. However, recent observations of island nucleation by irradiation with self-ions of Pt on Pt(111) do exhibit the symmetry predicted here.[30]

B. Magnitude of required μ^*

While the description of precipitation remains still to be perfected, the available treatments contain parameters that certainly possess the correct order of magnitude. It is therefore of interest that a treatment[12] of surface defect nucleation has specific predictions for the magnitude of μ needed to cause advacancy island nucleation. From the present perspective, this is the value of $\pm\mu^*$ needed to nucleate islands of the two signs; we further infer that the same results can be adapted to the bulk cases of dislocation loops. Concern centers on the predicted magnitude of the required μ^* and whether or not it conforms to the domain in which linear response theory is valid. This is the question considered in the present section. The differing distributions of precipitates

over the irradiated region in the Poisson and Frenkel pair regimes is a matter of further interest, deferred to Appendix E.

In the present notation the chemical potential μ_c^* predicted by Pimpinelli and Villain[12] for nucleation is $\mu_c^*/\pi a^2 > 0.2\beta^2/k_BT$, with a the atomic cell radius and β the energy per unit length of step edge. This gives

$$\frac{\mu_c^*}{k_BT} \approx \frac{s}{\bar{c}} \sim (\beta a)^2/2(k_BT)^2 \sim \frac{1}{5}. \tag{25}$$

Recent experiments on step fluctuations have shown that step edges have $\beta \sim 200$ meV/nm at high temperatures $\sim T_m/2$, on the close-packed surfaces of simple metals[31] with $T_m \sim 2000$ K; similar results are reported for Si (Ref. 32) at elevated temperatures. These values give rise to the numerical estimate given on the right of Eq. (25).

The result in Eq. (25) appears to confirm that the values, s/c, of fractional defect concentration required for island nucleation, under the stated high temperature conditions, are quite small, and fall within the expected regime of linear response. Note, however, that step energies are reported to be a factor of 3–10 larger at low temperatures, so that it could well be the case that linear response predictions fail below ~ 100 K. In the case of dislocation loops in the bulk, with dislocation energies[33,34] $\beta \sim 5$ eV/nm, and nucleation conditions probably fall outside the bounds of linear response at all temperatures up to T_m.

ACKNOWLEDGMENTS

The author thanks D. M. Ondrejcek for useful discussion and for assistance with the figures. This work was supported by the Department of Energy under Grant No. DE-FG02-02ER46011, and the Materials Research Laboratory of the University of Illinois, supported by Grant No. DEFG02-91ER45439.

APPENDIX A: SOLUTIONS FOR GEOMETRIES OF PRACTICAL INTEREST

Here the results of Sec. II are specialized to particular cases that have geometries of practical interest.

1. Solutions in one dimension

We consider the behavior in a domain of the variable x extending over $-l/2 < x < l/2$. Then $g_\kappa(x) = \cosh \kappa x$, $f(x) = [x^2 - (l/2)^2]/2$, and

$$D_1 s_1 = \frac{D_1\bar{c}_1(K_2 - K_1)[x^2 - (l/2)^2]}{2(D_1\bar{c}_1 + D_2\bar{c}_2)} + \frac{A}{\kappa^2}\left[\frac{\cosh \kappa x}{\cosh \kappa l/2} - 1\right];$$

$$D_2 s_2 = \frac{D_2\bar{c}_2(K_1 - K_2)[x^2 - (l/2)^2]}{2(D_1\bar{c}_1 + D_2\bar{c}_2)} + \frac{A}{\kappa^2}\left[\frac{\cosh \kappa x}{\cosh \kappa l/2} - 1\right]. \tag{A1a}$$

The same solution describes, in addition, processes on a 2D terrace of width l and infinite length, and also processes in a 3D rectangular slab of thickness l and of infinite extent in the other two dimensions.

2. Solutions in two dimensions

Solutions for a rectangular area follow from Eqs. (16) together with the separability of orthogonal dimensions. In this separation, identical values of κ^2 must be retained in each dimension, for each of which $\kappa^2/2$ must replace κ^2. Numerically, the factor is compensated by the increase in the D that occurs because the mean square displacement increases in proportion to dimensionality d.

Separate interest for 2D examples centers on the case of a circular boundary such as a terrace bounded by a step that forms a circle of radius R. Then $g_\kappa(r) = I_0(\kappa r)$, with I_0 the cylindrical Bessel function[24] of the first kind (finite at $r=0$) and zeroth order, for imaginary argument, and with $f(x) = [r^2 - R^2]/4$. Note that in the separation of the wave equation in circular coordinates that κ in the argument of the Bessel function in Eq. (10) is $\kappa^2 = \kappa_x^2 + \kappa_y^2$. The result is

$$D_1 s_1 = \frac{D_1\bar{c}_1(K_2 - K_1)[r^2 - R^2]}{4(D_1\bar{c}_1 + D_2\bar{c}_2)} + \frac{A}{\kappa^2}\left[\frac{I_0(\kappa r)}{I_0(\kappa R)} - 1\right];$$

$$D_2 s_2 = \frac{D_2\bar{c}_2(K_1 - K_2)[r^2 - R^2]}{4(D_1\bar{c}_1 + D_2\bar{c}_2)} + \frac{A}{\kappa^2}\left[\frac{I_0(\kappa r)}{I_0(\kappa R)} - 1\right]. \tag{A1b}$$

3. Solutions in three dimensions

Solutions for a rectangular block, and for a finite cylinder, follow directly from Eqs. (16) and (17) using the separability of the equations for orthogonal coordinates. Here we consider the case of a spherical volume, radius R, as a model, for example, of a crystalline grain isolated by a spherical grain boundary. Then $g_\kappa(r) = i_0(\kappa r)$, with i_0 the spherical Bessel function of the first kind of zeroth order, for imaginary argument,[24] and with $f(x) = [r^2 - R^2]/6$, so that

$$D_1 s_1 = \frac{D_1\bar{c}_1(K_2 - K_1)[r^2 - R^2]}{6(D_1\bar{c}_1 + D_2\bar{c}_2)} + \frac{A}{\kappa^2}\left[\frac{i_0(\kappa r)}{i_0(\kappa R)} - 1\right];$$

$$D_2 s_2 = \frac{D_2\bar{c}_2(K_1 - K_2)[r^2 - R^2]}{6(D_1\bar{c}_1 + D_2\bar{c}_2)} + \frac{A}{\kappa^2}\left[\frac{i_0(\kappa r)}{i_0(\kappa R)} - 1\right]. \tag{A1c}$$

APPENDIX B: DEFECT FLOW IN THE POISSON REGIME

Here we offer simple insight into behavior in the Poisson regime for dominant reactions. Consider a region of dimensionality d, extent R, containing $(R/a)^d$ particles, with a the particle radius. Then, in the steady state, $K(R/a)^d$ defects reach the boundary of area $\sim R^{d-1}$ each second, with $K = K_1 - K_2$. The flux density in the steady state is

$$J \sim KR/a^d; \tag{B1}$$

but the same flux density must also be given by the Nernst-Einstein equation:

$$J = (dDC/k_BT)\,\nabla\,\mu, \tag{B2}$$

with $C=c/a^d$ the concentration and dD the d-dimensional diffusion coefficient. Using

$$\nabla\mu \sim \mu(0); \quad c = c_1 + c_2; \quad f(0) \sim -R^2/d \tag{B3}$$

(see, e.g., Sec. II *C*); and

$$D = (D_1\bar{c}_1 + D_1\bar{c}_1)/(\bar{c}_1 + \bar{c}_2), \tag{B4}$$

one finds by equating the two expressions for J

$$\mu(0) = \frac{k_BT(K_1 - K_2)}{D_1\bar{c}_1 + D_2\bar{c}_2} f(0), \tag{B5}$$

just as in Eq. (23). Note in addition that the diffusion coefficient in Eq. (B4) can be derived more rigorously[22] for a system of reacting defects that obey the law of mass action. From this perspective, the result for strong reactions in Eq. (22) is just the behavior expected when products of the *completed* reaction drain to fixed sinks with the appropriate equilibrium diffusion coefficient.

APPENDIX C: SINK FLUCTUATIONS FROM GRADIENTS OF μ^*

It will often be the case that the perimeter of a driven volume is a defect sink, as in the cases discussed in Sec. III C. Examples are metal grains surrounded by grain boundaries and terraces contained between straight steps or enclosed within a surrounding step edge (e.g., a circular island of either sign). Questions then arise about the effect of the increased fluxes in amplifying fluctuations of the sinks themselves.

A simple example is the steady state rate at which a net excess of one defect over the other reaches a boundary. The answer is the rate at which new sites are created at the boundary is just the net excess of defects created in the enclosed region. Specifically, the excess is $(K_1-K_2)V/\Omega$ with V/Ω the number of sites enclosed. This determines, for example, the rate at which the region expands under the driving forces.

An interesting question concerns the total rate at which defects of either species attach to the boundary. The total rate per unit area (dimension $d-1$) determines the rate at which the boundary locus fluctuates in time. These boundary fluctuations can be formulated as a diffusion problem in the configuration space[27] of the boundary geometry, for which the time scale is the defect attachment rate. Antidefects of both type contribute simply in proportion to their attachment rates. The thermal equilibrium fluctuations occur on a time scale determined by the mass diffusion coefficient $D_1\bar{c}_1+D_2\bar{c}_2$. When the active region is driven by defect creation, the attachment rate is evidently increased by the excess defects reaching the boundary. It is then natural to enquire whether the resulting acceleration of boundary fluctuation rates can be employed as a means to monitor the net rate at which defects reach the boundary. In particular, with defects generated in a volume, and being deposited on a surface, it might seem that sufficiently large attachment rates might readily be achieved for large radii.

That this is not, in fact, the case, at least within the bounds of linear response, can be established by a simple argument presented here. The attachment rate at sink sites changes in proportion to the defect concentrations c at sites next to the boundary. In equilibrium, these take the values $\bar{c}_i$ that create the equilibrium attachment rates $D_i\bar{c}_i$ mentioned above. We see directly that the fractional *change* in attachment rate must be just $(c-\bar{c}_i)/\bar{c}_i$; but this change of concentration takes place over one atomic spacing in a system typically tens of nm or more in extent. It follows that to obtain fractional changes ~ 1 in the attachment rate at a boundary, the value of c near $r=0$ must be $\sim 10^2\bar{c}_i$ or larger. Such enormous changes correspond to very large driving forces that certainly fall outside the limitations of linear response. We conclude that sink fluctuations cannot offer a promising means for monitoring defect fluxes within the linear regime.

APPENDIX D: BULK AND SURFACE DEFECTS FOR TYPICAL METALS

The results employed above to estimate defect behavior in metals and on metal surfaces are those presented earlier[22] for use in other estimates. They are collected here for the convenience of the reader.

Mass diffusion.

Bulk: $\mathrm{D} = 0.3\,\exp(-17T_m/T)\mathrm{cm}^2/s;$

Surface: $\mathrm{D} = 5\times10^{-4}\,\exp(-6T_m/T)\mathrm{cm}^2/s.$ (D1)

Vacancy type defects.

Bulk: $D = 5\times10^{-2}\,\exp(-7T_m/T)\mathrm{cm}^2/s;$

$$\bar{c} = 6\,\exp(-10T_m/T)\mathrm{cm}^2/s; \tag{D2a}$$

Surface: $D = 3\times10^{-4}\,\exp(-2T_m/T)\mathrm{cm}^2/s;$

$$\bar{c} = 3\,\exp(-6T_m/T)\mathrm{cm}^2/s. \tag{D2b}$$

Added-atom type defects.

Bulk: $D = 10^{-4}\,\exp(-0.5T_m/T)\ \mathrm{cm}^2/s;$

$$\bar{c} = 10^7\,\exp(-30T_m/T)\mathrm{cm}^2/s; \tag{D3a}$$

Surface: $D = 2\times10^{-4}\,\exp(-1.5T_m/T)\mathrm{cm}^2/s;$

$$\bar{c} = 3\,\exp(-4.5T_m/T)\mathrm{cm}^2/s; \tag{D3b}$$

Mass action.

Bulk: $\bar{c}_1\bar{c}_2 = 6\times10^7\,\exp(-40T_m/T)\mathrm{cm}^2/s;$ (D4a)

Surface: $\bar{c}_1\bar{c}_2 = 9\,\exp(-10.5T_m/T)\mathrm{cm}^2/s.$ (D4b)

APPENDIX E: DISTRIBUTION OF NUCLEATION EVENTS

Since it is driven by excess chemical potential, nucleation is most probable where the change of μ^* caused by the driving forces is largest. For the natural geometries used in Sec. II C this occurs in the center of the sample, specifically where $x=0$ in one-dimensional cases, and where $\mathbf{r}=0$ in two and three dimensions (see Appendix A). The chemical potential elsewhere is smaller, since $s_i \to 0$ at the fixed boundary sinks. The point of further interest considered here is the spatial distribution of precipitates. This depends on the margin by which $\mu^*(0)$ exceeds the critical value $\mu_c^*(0)$ at which nucleation first takes place on experimental time scales, and so differs between the Poisson and Frenkel pair regimes.

Suppose then that the nucleation rate for a given excess $\delta\mu^* = \mu^* - \mu_c^*$ is given by

$$J = J_0 \delta\mu^*, \tag{E1}$$

which tends to zero with $\delta\mu^*$, as is reasonable. To specify $\delta\mu^*$ in a practical way, suppose that μ^* at $r=0$ exceeds μ_c by a fraction Δ. Thus

$$\mu_e^*(r) = \mu_c^*(1+\Delta)\mu^*(r)/\mu^*(0), \tag{E2}$$

with $\mu^*(r)/\mu^*(0)$ in general from Eq. (22). With $\mu(0)$ a maximum, the chemical potential can be expanded in a series about $r=0$ as

$$\mu_c^*(r) = \mu_c^*(0)(1 - \gamma r^2 + \cdots). \tag{E3}$$

From Eq. (E2), nucleation occurs only for $r < (\Delta/\gamma)^{1/2}$, and the mean square radius of nucleation events is now given approximately by

$$\langle r^2 \rangle = \int_0^{(\Delta/\gamma)^{1/2}} \mu_c(\Delta - \gamma r^2) r^{d+1} \mathrm{dr} \Big/ \int_0^{(\Delta/\gamma)^{1/2}} \mu_c(\Delta - \gamma r^2) r^{d-1} \mathrm{dr}$$

$$\sim d\Delta/(d+4)\gamma. \tag{E4}$$

Here, the dimensionality d determines how the volume element depends on radius r.

Interest now centers on values of β that describe particular experimental cases. In the Poisson limit, whether reaction or diffusion dominated, $\mu_c^*(r)/\mu_c^*(0) \sim (R^2 - r^2)/2d$ (see Sec. III C), so that $\gamma = R^{-2}$. Then

$$\langle r^2 \rangle \sim R^2 d\Delta/(d+4) \quad \text{(Poisson limit)}. \tag{E5}$$

This result is to be contrasted with the behavior in the limit of Frenkel pair creation. As the precise behavior depends on the particular geometry we employ, as a specific illustration the case $d=2$ of islands on a terrace, for which $\mu(r)/\mu(0) \sim [I_0(\kappa r)/I_0(\kappa R) - 1]$. For small r, $I_0(\kappa r) \sim 1 + (\kappa r)^2/2 + \cdots$, while for κR large,[35] $I_0(\kappa R) \sim (2\pi\kappa R)^{-1/2} \exp(\kappa R)$. We thus find for this case $\gamma \sim (2\pi R)^{1/2} \kappa^{5/2} \exp(-\kappa R)$. With γ thus exponentially small, the mean square radius in Eq. (E4) undergoes a commensurately large increase, and eventually at large κ, nucleation occurs everywhere except in a narrow band surrounding fixed sinks. In this way the observed distribution of precipitates may become a diagnostic for the system of reacting defects. The chemical potential in the Frenkel pair limit is much flatter at the system center than that in the Poisson as confirmed by the values of $\mu^*(r)/\mu^*(0)$ in Fig. 5. There, nucleation events occupy larger fractions of the active volume as κR increases, in agreement with Eq. (E4) above. The physical reason is that, in the Frenkel pair regime, the driving terms create no excess of either species, and little transport occurs from the center to perimeter sinks. μ^* is, accordingly, reduced. A gradient occurs near the perimeter, where an imbalance over a distance $\sim \kappa^{-1}$ is caused by differing transport to sinks of the two species. In the Poisson regime, in contrast, the gradient drives excess defects to perimeter sinks and the precipitates are less disperse.

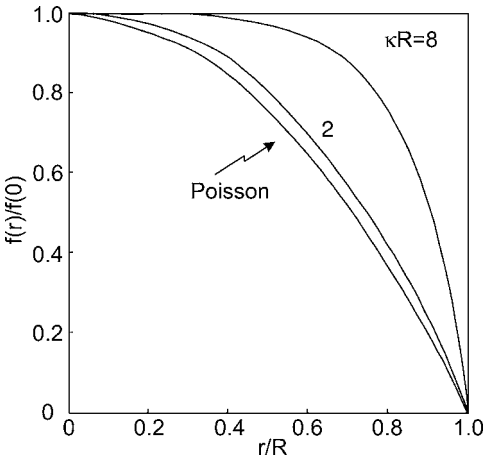

FIG. 5. The fractional variation of μ^* with radius r $(0 < r < R)$ for the Poisson solution in Eq. (23a), and the Frenkel pair case, indicated for two values of κR, showing first how they are identical for $\kappa \to 0$, and second, the flatter distribution near $r=0$ for $\kappa R \gg 1$.

[1] Y. Adda and J. Phillibert, *La Diffusion dans les Solides* (Universitaires de France, Paris, 1966).

[2] C. P. Flynn, *Point Defects and Diffusion* (Oxford Press, Oxford, 1972).

[3] A. B. Lidiard, *Handb Phys 20* (Springer, Berlin, 1957).

[4] A. Pimpinelli and J. Villain, *Physics of Crystal Growth* (Cambridge University, Cambridge, England, 1998).

[5] A. Zangwill, *Physics at Surfaces* (Cambridge University, Cambridge, England, 1998).

[6] H.-C. Jeong and E. D. Williams, Surf. Sci. Rep. **34**, 171 (1999).

[7] M. Geisen, Prog. Surf. Sci. **68**, 1 (2001).

[8] C. P. Flynn, Phys. Rev. B **73**, 155417 (2006).

[9] F. Seitz and J. S. Koehler, *Solid St Phys* Vol. 2 (Academic Press, New York, 1956).

[10] G. J. Dienes and G. H. Vineyard, *Radiation Effects in Solids* (Interscience, New York, 1957); M. W. Thompson, *Defects and*

Radiation Damage in Metals (Cambridge University, Cambridge, England, 1969).
[11] R. S. Averback and T. D. de la Rubia, *Solid State Physics* Vol. 51 (Academic Press, New York, 1998), p. 281.
[12] A. Pimpinelli and J. Villain, Physica A **204**, 521 (1994).
[13] *Fundamentals of Radiation Damage*, edited by I. M. Robertson, R. S. Averback, D. K. Tappin, and L. E. Rehn (North-Holland, Amsterdam, 1994).
[14] J. Silcox and P. B. Hirsch, Philos. Mag. **4**, 72 (1959).
[15] See, e.g., R. Bullough and R. S. Nelson, Phys. Technol. **5**, 1 (1974).
[16] J. W. Evans, P. A. Thiel, and M. C. Bartelt, Surf. Sci. Rep. **61**, 1 (2006).
[17] T. Michelly and J. Krug, *Islands, Mounds and Atoms* (Springer, Berlin, 2004).
[18] C. Alphonso, J. M. Bermond, J. C. Heyraud, and J. J. Metois, Surf. Sci. **262**, 371 (1992).
[19] S.-J. Tang, S. Kodembaka, W. Sweich, I. Petrov, C. P. Flynn, and T.-C. Chiang, Phys. Rev. Lett. **96**, 126106 (2006).
[20] N. V. Doan and G. Martin, Phys. Rev. B **67**, 134107 (2003).
[21] J. P. Beirsack and I. G. Haggmark, Nucl. Instrum. Methods **174**, 257 (1980).
[22] C. P. Flynn, Phys. Rev. B **71**, 085422 (2005).
[23] R. Sizmann, J. Nucl. Mater. **69-70**, 385 (1978).
[24] See, e.g., P. M. Morse and H. Feshbach, *Methods of Theoretical Physics* (McGraw-Hill, New York, 1953).
[25] R. Becker and W. Doring, Ann. Phys. **24**, 719 (1935).
[26] D. Turnbull and J. C. Fisher, J. Chem. Phys. **17**, 71 (1949).
[27] C. P. Flynn, Phys. Rev. B **66**, 155403 (2003).
[28] P. Ehrhart, *Landolt-Bornstein New Series, Group III, Vol. 25* edited by H. Ullmaier (Springer, Berlin, 1991), p. 115.
[29] M. Mundschau, E. Bauer, W. Teleips, and W. Swiech, Surf. Sci. **223**, 413 (1989).
[30] C. P. Flynn, M. Rajappan, W. Sweich, and M. Ondrejcek (unpublished).
[31] M. Ondrejcek, M. Rajappan, W. Swiech, and C. P. Flynn, Phys. Rev. B **73**, 035418 (2006); M. Ondrejcek, W. Swiech, and C. P. Flynn, *ibid.* **72**, 085422 (2005).
[32] N. C. Bartelt and R. M. Tromp, Phys. Rev. B **54**, 11731 (1996).
[33] J. P. Hirth and J. Lothe, *Theory of Crystal Dislocations* (Wiley, New York, 1982).
[34] R. N. Nabarro, *Theory of Crystal Dislocations* (Dover, New York, 1987).
[35] I. S. Gradshteyn and I. M. Ryzhic, *Tables of Integrals, Series and Products* (Academic Press, New York, 1980).